Dielectric Relaxation and Crystallization Kinetics of Ibuprofen at Ambient and Elevated Pressure

K. Adrjanowicz,* K. Kaminski, Z. Wojnarowska, M. Dulski, L. Hawelek, S. Pawlus, and M. Paluch

Institute of Physics, University of Silesia, Uniwersytecka 4, 40-007 Katowice, Poland

W. Sawicki

Department of Pharmaceutical Technology, Medical University of Gdansk, Hallera 107, 80-416, Gdansk, Poland

Received: October 19, 2009; Revised Manuscript Received: February 11, 2010

Dielectric spectroscopy (DS) was used to investigate the relaxation dynamics of supercooled and glassy ibuprofen at various isobaric and isothermal conditions (pressure up to 1750 MPa). The ambient pressure data are in good agreement with that reported previously in the literature. Our high pressure measurements revealed validity of temperature−pressure superpositioning (TPS) for the α-peak. We also found that the value of the fragility index decreases with compression from $m = 87 \pm 2$ at atmospheric pressure to $m = 72.5 \pm 3.5$ at high pressure ($p = 920$ MPa). The drop of fragility observed in our experiment was discussed in the framework of the two-order-parameter (TOP) model. In addition, we have also studied crystallization kinetics in a liquid state of examined drug at ambient and high pressure. We found out that, for the same structural relaxation time/same viscosities, the samples prepared by compression of liquid at high temperatures have significantly elongated induction times as well as overall crystallization times (sample 2: $t_0 \cong 4$ h, $t_{1/2} \cong 37.5$ h; sample 3: $t_0 \cong 5.6$ h, $t_{1/2} \cong 49$ h) compared to that held at lower temperature and ambient pressure (sample 1: $t_0 \cong 1.2$ h, $t_{1/2} \cong 12.2$ h). A possible explanation of this finding is also given.

1. Introduction

Ibuprofen (2-[4-(2-methylpropyl)phenyl]propanoic acid) is a nonsteroidal antiflamamatory drug. It was discovered in the 1960s in the U.K. and until nowadays is indicated for the relief of pain and fever by millions of people in the whole world. The experimental solubility of ibuprofen in water (0.049 mg/mL[1]) enables this medicine to be classified as almost insoluble in water. In the case of such a drug, the dissolution profile and bioavailability after oral administration are relatively low.[2,3]

One of the well established methods for increasing the solubility and bioavailability of poorly water-soluble drugs is preparing them in the amorphous form. Unlike their crystalline counterparts, amorphous pharmaceuticals are markedly more soluble, they have greater dissolution profiles, and their bioavailability can also be improved.[4–6] Moreover, it was recently reported that in some cases amorphous drugs compact into tablets much better than crystalline,[7] which may give an opportunity for pharmaceutical companies to omit addition of the excipients, commonly used to shape drugs into tablets.

Although, mentioned above benefits given by the amorphous state, one should still remember that the amorphous solid is an out of equilibrium state (its properties change with time). Because of that reason, amorphous drugs would revert to a more stable crystalline form. From a pharmaceutical point of view, an amorphous drug produced for commercial use should maintain physically stable for a typical shelf life (at least 3 years). Of course, some of them are more stable against crystallization and others less.[8,9] Moreover, in some cases (like indomethacin), even storage at a temperature of 50 K below the T_g might not be sufficient to avoid crystallization.[10,11]

Due to the high instability of the amorphous form, production and commercial use of the amorphous pharmaceuticals have been significantly curbed. In agreement with the latest reports, understanding of the crystallization from the amorphous state and its relationship with molecular mobility seems to be very important to produce stable amorphous drugs.[9,11–14] In the past few years, especially a lot of attention was paid to local molecular mobility involved with the JG relaxation. For example, as shown by the Oguni group, the crystal growth rate near T_g is controlled by the β-process rather than the α-process.[15–18]

Current research also shows that ably control amorphization may lead to highly stable glassy drugs. Because of high densities (lower molecular mobility) and lower water uptake they do not crystallize so easily and are appropriate new drug candidates. Typically, glasses are prepared by cooling of a liquid. Alternatively, they can also be prepared from solutions (spray[19] and freeze-drying[6]), from solid state (grinding[20] or pressurization of crystals[21]), by compression of liquid,[22] and by vapor deposition.[23] Such a large variety of methods allowed amorphization of almost every kind of material. However, it should also be noted that the way of amorphization influences the physical stability of the material.[24] Glasses prepared using various methods have sometimes completely different enthalpies and densities.[25] For example, the glassy state of indomethacin obtained by very slow cooling of a liquid is stable against crystallization over 2 years,[26] but the amorphous state of IMC obtained by cryogenic grinding is less stable and recrystallizes to 90% after approximately 13−15 h.[20,27] The more interesting

* Corresponding author. E-mail: kadrjano@us.edu.pl.

10.1021/jp910009b
Published on Web 04/23/2010

results have been recently obtained by Ediger's group. They showed that highly stable amorphous indomethacin can be obtained by vapor deposition.[23,25,28] Interestingly, by controlling the substrate temperature during the deposition of indomethacin, it is possible to prepare glass with lower enthalpy, greater density, and initially kinetic stability comparable to that produced by aging of ordinary glass for 7 months.[25] What is more, stable glass absorbs 5 times less water than that obtained by the traditional way,[29] since the free space available for water molecules has been reduced in it to the absolute minimum. This highly stable glass seems to have very important applications in many fields of science, also for pharmaceutical industry.

The latest research done by our group clearly showed that, except physical vapor deposition stable glasses can be prepared by application of a high pressure. While it was previously reported for some (nonpharmaceutical and pharmaceutical) glass-formers[30–33] using specific thermodynamic pathways, it is possible to get an amorphous form with higher density. When the glass transition occurrs at higher temperature and pressure, a glass is characterized by denser molecular packing. This situation is manifested in the increase of relaxation times τ_β as well as the activation energy of the β-process.[30] In addition, we have experimentally observed that compression of supercooled triphenyl phosphite (TPP) and indomethacin suppress crystallization and causes decrease of the fragility index.[32,34] The latter result is being experimental support of the Two-Order Parameter model (TOP).

The TOP model[35–37] was proposed by Tanaka to explain the liquid−glass transition. In his explanation of the glass transition, it is being controlled by competition (energetic frustration) between long-range density ordering toward crystallization and short-range bond ordering toward formation of locally favored structures. In accordance with the TOP model, besides kinetic factors (viscosity), energetic frustration also plays a key role in preventing the crystallization. The scale of this frustration is related to the bond order parameter S, given by the following equation

$$\bar{S} \cong S_0 \exp[\beta(\Delta E - p\Delta v)] \quad (1)$$

where $\bar{S}$ is the average value of S, $\beta = 1/k_B T$, p is the pressure, and ΔE and Δv are the energy gain and the specific volume change upon the formation of a locally favored structure, respectively. The TOP model predicts that the frustration between these two types of density ordering in the liquid state controls its fragility. In other words, for stronger liquids, stronger frustration occurred, while, for more fragile liquids, frustration was weaker ($S \rightarrow 0$). On the basis of the above equation, if we apply high pressure, the bond parameter increases; the frustration of the system also increases and the liquid becomes stronger. As a consequence, the reduction of fragility should improve the stability of the system against crystallization below the T_g.

Here, we reported dielectric measurements at ambient and elevated pressure of ibuprofen. Dielectric relaxation and crystallization of this drug at ambient pressure were studied recently by Johari et al.[38] and Brás et al.[39] The latter one showed the existence of the intermolecular hydrogen-bonded aggregates (dimers or trimers) formed by ibuprofen molecules which favor antiparallel correlation of the dipole vectors. Of key interest for this paper is the molecular dynamics in the examined drug under different thermodynamic conditions. In accordance with the Tanaka model, we observed a significant decrease of the fragility index after application of high pressure. Thus, we expect that denser glassy ibuprofen should be more stable against crystallization than that obtained by the ordinary way (supercooling of liquid). Finally, we have also studied the crystallization kinetics of supercooled ibuprofen at ambient and high pressure. In the Results and Discussion section, we will show experimental proof that high pressure is the best tool to significantly slow down the crystallization development and extension of its induction time.

2. Experimental Section

2.1. Material. Ibuprofen (being a racemic mixture of (*S*)-ibuprofen and (*R*)-ibuprofen) of greater than 98% purity was supplied from Hubei Biocause Pharmaceutical Co. Ltd. and used as received. One can find the chemical structure of the *R* and *S* enantiomers in ref 39. The starting material was completely crystalline with a melting point of 348 K, which agrees with that reported in the literature (348−350 K)[40] and references therein.

2.2. Method. ***2.2.1. Dielectric Spectroscopy.*** Isobaric dielectric measurements at atmospheric pressure were carried out using a Novocontrol GMBH Alpha analyzer (10^{-2}−10^6 Hz) and a Quatro temperature controller with a temperature stability better than 0.1 K. The sample was placed between two stainless steel electrodes (diameter 15 mm, 0.1 mm gap maintained by use of the Teflon spacer). In case the of ambient pressure studies, to ensure a complete melting, the sample was kept 10 K above its melting temperature (T_m = 348 K) for about half an hour and after that fast cooled (10 K/min) in order to its vitrification. Dielectric spectra of ibuprofen measured at atmospheric pressure were collected from 133 to 263 K in different steps: 133 to 193 K in steps of 10 K, 193 to 223 K in steps of 5 K, and 225 to 263 K in steps of 2 K.

For high pressure studies, we used a Unipress system, with a special homemade flat parallel capacitor. Thin Teflon spacers were used to maintain a fixed distance between the plates. The sample and the two electrodes forming a capacitor were placed in a Teflon bellows mounted in the high pressure chamber. Pressure was exerted via a steel piston and hydraulic press. This technique enables us to generate pressures of the order of a few gigapascals. Pressure was measured by a Nova Swiss tensometric pressure meter with an accuracy of 10 MPa. The temperature of the high pressure cell in the range from 383 to 263 K was controlled to within 0.1 K by a thermostatic bath and from 263 to 218 K by an environmental chamber with identical accuracy. A representative illustration of this experimental setup and more detailed information about experimental equipment are described in ref 41.

We have performed isobaric measurements at p = 920 MPa and p = 1750 MPa in the temperature ranges 337−373 and 218−358 K, respectively. The latter isobar (p = 1750 MPa) was measured in order to check the effect of pressure on the secondary relaxations. Moreover, we have also carried out isothermal measurements at T = 293 K and T = 378 K under increasing pressure from p = 162 MPa to 425 MPa and p = 920 MPa to 1750 MPa, respectively.

Crystallization kinetics studies of ibuprofen were carried out for three sets of pressure and temperature combinations but for approximately the same structural relaxation times ($\tau_\alpha \approx 1 \times 10^{-5}$ s)/ same viscosities of the samples. Sample 1 was kept at ambient pressure and temperature, T = 255 K, the second one at p = 550 MPa and T = 343 K, and the last one at p = 920 MPa and T = 383 K. The crystallization kinetics studies presented in this paper have been performed using the same experimental environment (the high pressure cell described

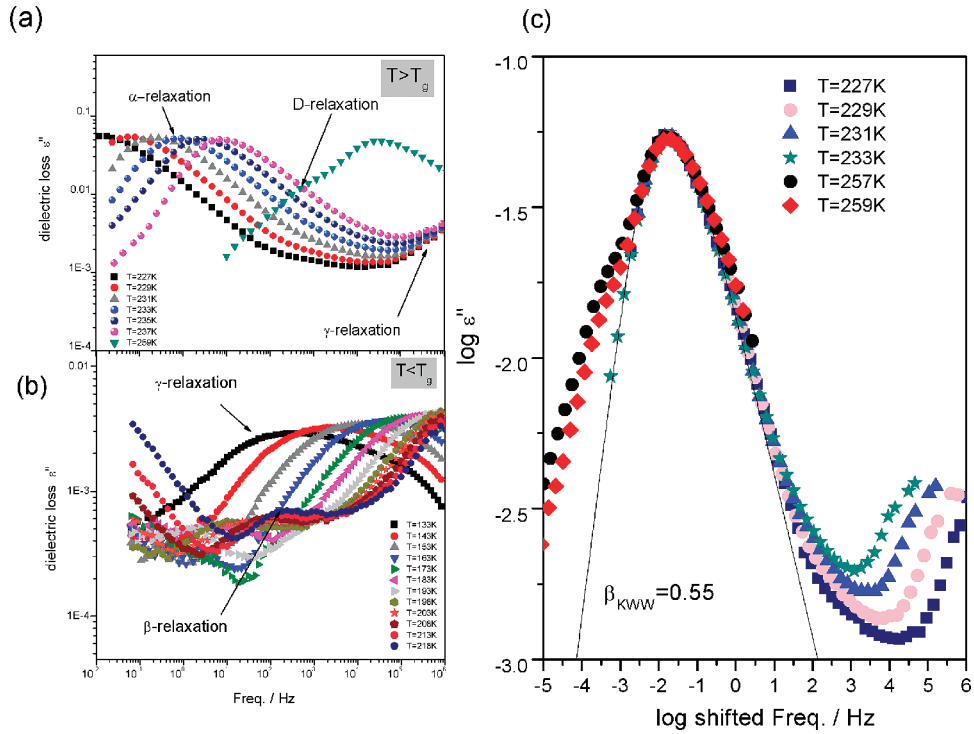

Figure 1. (a and b) Dielectric loss spectra of ibuprofen measured above and below its glass transition temperature at ambient pressure. The $\varepsilon''(f)$ dependences were collected during heating from 133 to 263 K in different steps: 133−193 K in steps of 10 K, 193-223 K in steps of 5 K, and 225−263 K in steps of 2 K. (c) Master plot of ibuprofen constructed by horizontal shift of several selected loss spectra collected above T_g, to overlap with the spectrum taken at $T = 227$ K. The black solid line represents the KWW fit of the α-peak at 227 K with $\beta_{KWW} = 0.55$.

above). This procedure ensures the most reliable comparison between data coming from various thermodynamic conditions. In all cases, during the measurements, the sample was in contact only with the stainless steel electrodes (of the same surface) and Teflon spacer. Each sample (3.5 g) was annealed for about 1 h at 20 K above the melting temperature, to ensure that there was no crystallinity. For crystallization kinetic studies at high pressure before the first spectrum was collected, we waited about 10 min to stabilize the experimental conditions. The real and imaginary parts of the complex permittivity were measured every 600 s within the same frequency range (100 Hz to 3 MHz). Thus, each spectrum was collected in a time that did not exceed 1 min, which guaranteed that during a measurement the change in crystallinity of a sample was significantly small. All crystallization experiments were performed in duplicate. In the case of crystallization carried out at ambient pressure (sample 1), to avoid impractically long induction times, the spectra were collected in the temperature region where the most favorable nucleation and crystal growth rate occur. As shown by Dudognon and co-workers[42] for conventional ibuprofen at ambient pressure, such a temperature region is located between 233 and 263 K. However, we have also performed our own measurements. To find the most suitable induction time t_0 (reasonably short) for the sample crystallized at ambient pressure, we have monitored by dielectric spectroscopy (DS) the α-relaxation peak at several temperatures between 247 and 267 K. On the basis of the findings of Dudognon and co-workers as well as our own observations, we have selected the temperature $T = 255$ K for which the induction time took roughly an hour. For samples 2 and 3, the temperature and pressure were carefully selected so that their structural relaxation times closely match that taken at ambient pressure ($T = 255$ K).

2.3. Additional Techniques. ***2.3.1. Infrared Spectroscopy (IR).*** Transmission infrared spectra were measured using a Bio-Rad FTS-6000 spectrometer equipped with an infrared microscope of the Bio-Rad UMA-500 type with grazing angle objective and Panasonic GP-KR 222 camera. The microscope had its own 250 mm × 250 mm mercury cadmium telluride detector (MTC) cooled to 77 K using liquid nitrogen. The spectra were obtained in the range 3500−500 cm^{-1} with a resolution of 4 cm^{-1}. The interferograms were recorded by accumulating 128 scans, and a gold-covered microscope slide was used to obtain the background spectra.

2.3.2. X-ray Powder Diffraction (XRPD). The X-ray diffraction experiment was performed at ambient temperature and pressure on a Rigaku-Denki D/MAX RAPID II-R diffractometer with a rotating anode Ag Kα tube ($\lambda = 0.5608$ Å), an incident beam (002) graphite monochromator, and an image plate in the Debye−Scherrer geometry. The pixel size was 100 μm × 100 μm. Both samples were placed inside Lindemann glass capillaries (2 mm in diameter); measurements were performed for the sample filled and empty capillaries, and the intensity for the empty capillary was then subtracted. The beam width at the sample was 0.1 mm. The two-dimensional diffraction patterns were converted into the one-dimensional intensity data using suitable software.

3. Results and Discussion

3.1. Ambient Pressure Data. Figure 1 shows dielectric loss spectra of ibuprofen measured at atmospheric pressure above (panel a) and below (panel b) the glass transition temperature T_g, defined as a temperature at which the structural relaxation time is equal to 100 s.

Our own dielectric measurements taken at ambient pressure confirmed the existence of multiple relaxation processes reported earlier in the literature. At the lowest temperatures, deep in the glassy state, there is a well-defined secondary relaxation, the γ-relaxation. It is interesting to point out that this mode is asymmetric. It is opposite to the common rule. As the temperature increases, another secondary relaxation, with much smaller

amplitude, appears. We designed it as the β-relaxation. It is the most visible between 198 and 223 K. Above the glass transition, this process becomes hidden by the main α-relaxation. Consequently, it is reflected as a change in slope of the high frequency side of the structural relaxation peak in dielectric loss spectra. In the supercooled state of ibuprofen, there is also another process, slower than the α-relaxation. It appears at lower frequencies than the structural relaxation peak and was labeled as a D-process.[39] The prominent Debye-type dielectric relaxation is a common feature to many monohydroxy alcohols in their liquid state.[43–45] What is more, for a large variety of alcohols, the dielectric strength of the Debye process is even higher than the α-process. In the case of ibuprofen, the dielectric strength of the Debye process is considerably smaller than the main α-relaxation.

The previous studies of ibuprofen confirmed its strong tendency to form noncovalent bonding aggregates. As a result of intermolecular interaction in the solution, two ibuprofen molecules, associated via hydrogen bonds, formed a dimer structure $[2Ibu-H]^-$. The existence of trimer structures was also reported. Hence, it was suggested that appearance of the D-process is associated with hydrogen-bonded cyclic structures.[39]

From our observations, we have also noticed that appearance of the D-relaxation in ibuprofen strongly depends on the thermal history of the sample. According to how long and at what temperature the sample was annealed to ensure a complete melting, the D-process appears more visible or only as a slight broadening of the low frequency part of the α-peak, seen about 4 decades below the maximum of the structural relaxation peak. In the case of the latter situation, determination of the most probable relation times τ_D of the D-process was fairly impossible. For detailed studies of the $\tau_D(T)$ dependence, we would like to refer readers to the publication of Brás and co-workers.

Interestingly, we also have noticed that, when the sample was annealed just for a while (less than 5 min) slightly above the melting temperature and after that fast cooled, the D-like process was not observed in the loss spectra. The D-relaxation was also not detected when the sample was cooled from 373 K (after a few minutes of warming at that temperature). On the contrary, the ibuprofen kept for about 2 h at 373 K and after that fast cooled (with a rate of ~30 K/min) to its supercooled state revealed in loss spectra the D-relaxation peak. A more detailed discussion on the influence of the thermal history of the sample on the appearance of the D-peak is beyond the aim of this paper. We planned some studies on that finding in the future. Despite that, it is worth remembering that the contribution of the D-relaxation to the structural relaxation process can be neglected.

In Figure 1c, we present a master curve. It was obtained by horizontal shift of a few arbitrarily chosen spectra (taken at different temperatures above T_g, from 229 to 259 K) to superpose all together with the unshifted data at 227 K. As can be seen, the shape of the structural peak in that temperature range is essentially invariant to the temperature change. Next, we fitted the α-loss peak taken at a temperature of $T = 227$ K by the one-side Fourier transforms of the Kohlrausch−Williams−Watts (KWW) function[46]

$$\varphi(t) = \exp[-(t/\tau_\alpha)^{\beta_{KWW}}] \tag{2}$$

with $\beta_{KWW} = 0.55$. This value is comparable with $\beta_{KWW} = 0.54$ reported by Johari.[38]

Relaxation times of the α-, β-, and γ-processes were determined from the frequency maximum of the loss peaks and

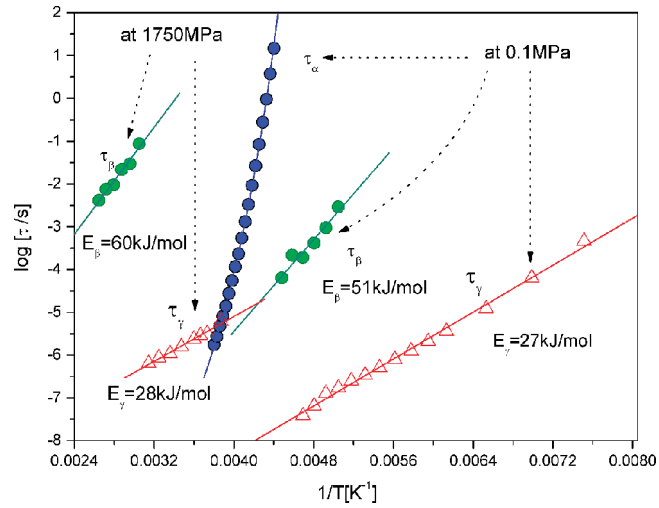

Figure 2. Relaxation map of ibuprofen. The temperature dependence of the structural relaxation time α (blue circles) at 0.1 MPa was described by the VFT equation (blue line). Green circles denote β-relaxation times obtained at ambient (0.1 MPa) and high pressure ($p = 1750$ MPa). Red open triangles denote the γ-relaxation times obtained at ambient (0.1 MPa) and high pressure ($p = 1750$ MPa). Respective β- and γ-relaxation times are shown by the arrows. To fit the temperature dependence of secondary relaxations, β and γ, we used the Arrhenius equation; these fits for β- and γ-relaxation times are marked as green and red lines, respectively.

plotted versus the inverse of temperature, as shown in Figure 2. The temperature dependence of the α-relaxation was fitted to the Vogel−Fulcher−Tamman (VFT) equation[47]

$$\log_{10}\tau_\alpha = \log_{10}\tau_0 + \frac{(DT_0)}{T - T_0} \tag{3}$$

with $\log_{10}\tau_0 = -14.8 \pm 0.2$ s, $D = 4.2 \pm 0.2$, and $T_0 = 181 \pm 1$ K. From the VFT fits, the glass transition temperature was estimated as $T_g = 225$ K and the fragility index m was calculated

$$m = \left.\frac{d\log_{10}\tau_\alpha(T)}{d(T_g/T)}\right|_{T=T_g} \tag{4}$$

It leads us to $m = 87 \pm 2$, indicating that ibuprofen is a moderately fragile glass former. It is worth pointing out that T_g determined from our dielectric data agrees well with that determined by Johari et al. ($T_g = 223$ K)[38] and Brás et al. ($T_g = 226$ K).[39] On the other hand, the fragility of ibuprofen determined by us is slightly different from that previously reported in the literature. Brás et al. estimated $m = 93$[39] using the same procedure as we did. However, their fragility index was calculated on the basis of the temperature dependence of the structural relaxation times not longer than 1 s (for a relaxation map of ibuprofen, see Figure 12 of ref 39). On the other hand, we have estimated the steepness index for the relaxation times measured up to 20 s. Consequently, with extrapolation of the VFT fit to 100 s (T_g), we are making less error than they did. Hence, here we can find the source of discrepancy in estimation of the fragility of the ibuprofen by us and Brás et al. Since our structural relaxation times are almost 1.5 decades longer than that provided in ref 39, we think the fragility index of ibuprofen given in our paper is even more accurate.

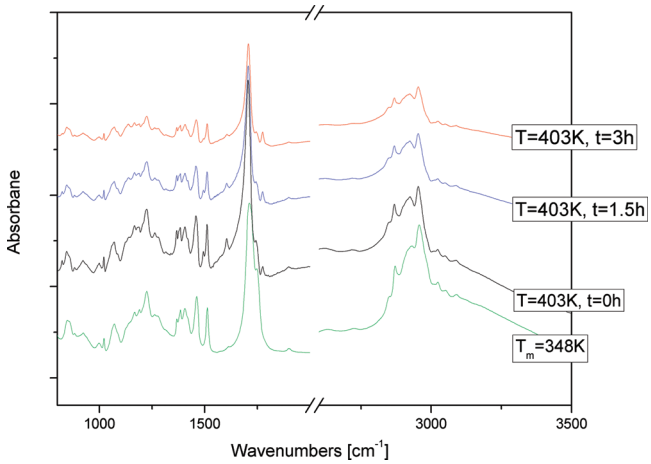

Figure 3. FTIR spectra of ibuprofen collected at 348 and 403 K after $t = 0$ h, $t = 1.5$ h, and $t = 3$ h of annealing.

The temperature dependences of the relaxation times of both secondary modes exhibit a linear dependence and can be well-described by the Arrhenius equation

$$\tau(T) = \tau_0 \exp\left(\frac{E_a}{RT}\right) \quad (5)$$

with $\tau_0 = 7 \times 10^{-17}$ s, $E_\beta = 51 \pm 4$ kJ/mol for the β-relaxation and $\tau_0 = 1.7 \times 10^{-14}$ s, $E_\gamma = 27 \pm 0.5$ kJ/mol for the γ-relaxation. The activation barriers for both secondary relaxations agree with those found in the literature ($E_\beta = 52 \pm 2$ kJ/mol and $E_\gamma = 30.5 \pm 0.7$ kJ/mol[39]).

Recently, the molecular origin of both secondary relaxation processes was investigated. It turned out that the faster secondary relaxation process is related rather to the very local motions of the part of the ibuprofen molecule. In ref 39, this process was assigned to the movements of the carboxylic group. On the other hand, the slower relaxation mode (β) was classified as a true Johari−Goldstein (JG) relaxation. However, it should be stressed that Brás et al. applied the coupling model (CM) to identify the molecular origin of the secondary relaxations in ibuprofen.[39] At this point, it should be added that the CM is only a theoretical tool which is very useful in finding true JG relaxation in different kinds of materials.[48,49] On the other hand, there is also another experimental way which can verify CM predictions. It is well-known that the JG relaxation process should be sensitive to pressure just as the structural relaxation mode is. Thus, to check whether the slow secondary relaxation is of intermolecular origin further pressure measurements were done.

3.2. Elevated Pressure Data. Our dielectric relaxation measurements carried out at elevated pressure as well as described in the further part of this paper crystallization kinetics studies were performed at high temperatures, even up to 383 K. Thus, a question may arise: are they not affected by thermal decomposition? As can be found in the literature, ibuprofen is thermally stable up to 453−473 K.[50,51] Nevertheless, before dielectric measurements were started, additional IR measurements were done to prove that prolonged thermal treatment did not affect our sample. In the first step, the sample was heated up to the melting point ($T_m = 348$ K) where the transmittance IR spectrum was collected. After that, the sample was heated to 403 K (that is, 20 K higher than in our pressure measurements). The spectra were recorded every 15 min for 3 h. The results are presented in Figure 3. As can be seen, even long-term exposition of ibuprofen for high temperatures does not modify the initial structure. The decrease of intensity of the main bands with time can be explained by mass loss caused by slow evaporation of ibuprofen at this temperature.[40] Analysis of recorded spectra allowed us to confirm that at high temperature ibuprofen will not undergo thermal degradation in the studied range of temperatures.

We have performed isothermal and isobaric dielectric relaxation measurements under high temperature and pressure conditions. It is worth noting that a study of the molecular dynamics of ibuprofen at elevated pressure has not been done before. We have carried out isothermal measurements at $T = 293$ K and $T = 378$ K under pressure increasing from $p = 162$ to 425 MPa and $p = 920$ MPa to 1750 MPa, respectively. The isobaric measurements were conducted at $p = 920$ MPa and $p = 1750$ GPa in the temperature ranges 337−373 and 218−358 K, respectively. However, the latter isobar ($p = 1750$ MPa) was measured in order to check the effect of pressure on the secondary relaxations. For sake of clarity in Figure 4, we present only representative isothermal (panel a) and isobaric (panel b) dielectric loss spectra of ibuprofen. As can be seen in Figure 4, upon both decreasing temperature and increasing pressure, the structural relaxation slows down. The α-peak exhibits strong sensitivity to pressure; less than 600 MPa is enough to move it through the experimentally available frequency range. At higher frequencies (10^5−10^6 Hz), the low frequency side of the γ-relaxation is observed. Isothermal measurements at $T = 378$ K (Figure 4a) clearly demonstrate that the γ-process seems to be insensitive to applied pressure. One can see that compression of liquid brings about a shift by many orders of magnitude of the structural relaxation peak, while the position of the γ-relaxation peak remains unchanged. It is worth noting that the sensitivity to pressure is one of the most important criteria used to classify the secondary relaxation as a "genuine" JG process.[52] For ibuprofen, the pressure invariance of the γ-peak indicates this secondary relaxation as a non-JG process.

Similar as for the data taken at ambient pressure, above the glass transition, the β-relaxation process is being submerged by the main α-process. This relaxation becomes visible in the glassy state, as seen in Figure 5 for isobar $p = 1750$ MPa. Analysis of the collected data, in the temperature range between 378 and 218 K, allowed us to calculate the activation energies of both secondary relaxations. The temperature dependence of relaxation times τ_β and τ_γ (which were also included in the relaxation map of ibuprofen (Figure 2)), fitted to the Arrhenius equation, gives the following values of activation barriers for both modes: $E_\beta = 60 \pm 4$ kJ/mol and $E_\gamma = 28 \pm 1$ kJ/mol for β-relaxation and γ-relaxation, respectively. As we expected, the activation energy for the γ-process practically does not change when compared to the ambient pressure value ($E_\gamma = 27 \pm 0.5$ kJ/mol). This is another sign of the local, non-JG nature of the γ-relaxation. As suggested by Brás and co-workers,[39] for occurrence of this type of motion might be responsible fluctuation of carboxylic groups, which at low temperatures can form effective hydrogen bonds. It is interesting to note that the activation barrier for the β-relaxation under high pressure just slightly increases ($E_\beta = 51 \pm 4$ kJ/mol at 0.1 MPa). This situation reflects the density variation of glasses formed using different thermodynamic pathways. Here, we would like to refer readers to our previous works,[30−33] where we clearly showed that vitrification of liquid by compression at high temperature usually leads to denser glass than cooling. The effect of glass

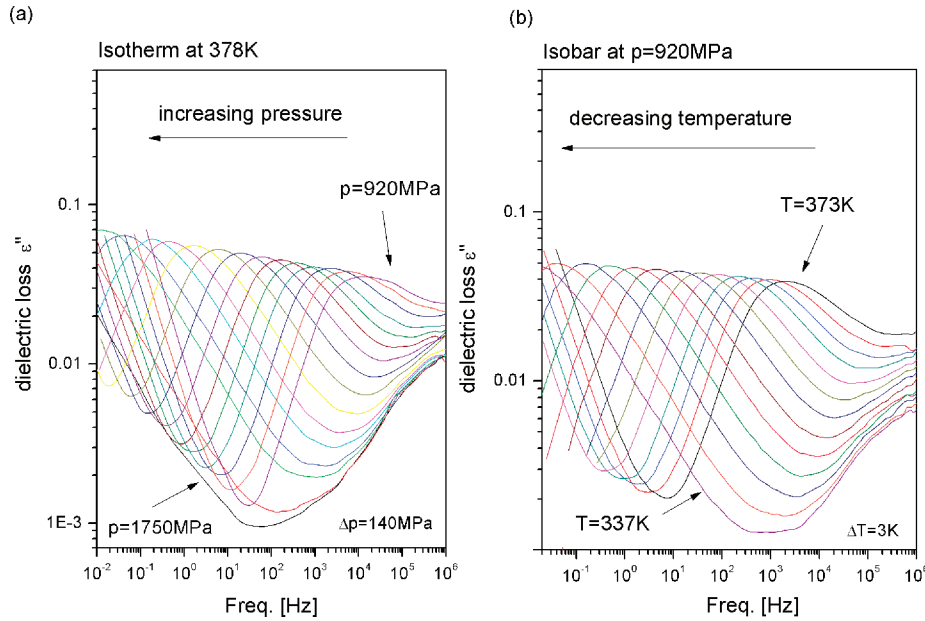

Figure 4. Representative dielectric loss data obtained at two different combinations of temperature and pressure. Panel a presents loss spectra collected during isothermal measurements carried out at $T = 378$ K under applied pressures increasing from $p = 920$ MPa up to 1750 MPa. Panel b presents dielectric loss spectra measured during isobaric measurements at $p = 920$ MPa and various temperatures in the range 373−337 K in steps of 3 K.

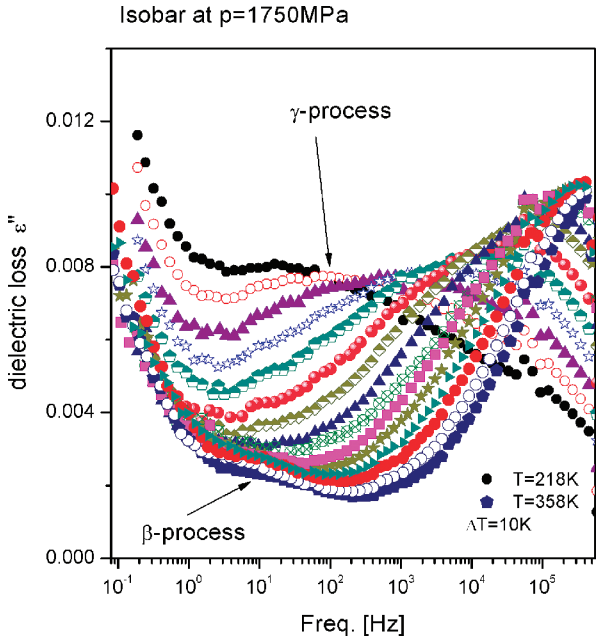

Figure 5. Dielectric loss spectra obtained from isobaric measurements at $p = 1750$ MPa and various temperatures in the range between 358 and 218 K, with steps of 10 K.

structure is manifested in the increase of activation energy for the β-relaxation. We speculate a similar scenario for ibuprofen.

Taking into account the behavior of the β-relaxation under high pressure, it has been identified by us as an intermolecular Johari−Goldstein process. The discussion given in this section about the nature of the secondary relaxations in ibuprofen seems to be complementary to that given by Brás and co-workers,[39] since their interpretation of the JG process is based only on the CM criterion. Ibuprofen has a strong tendency to create hydrogen-bonded cyclic structures; thus, it would be interesting to check whether the increase of pressure reduces their concentration or not. Despite the long history, the effect of pressure on hydrogen bonding is not clear and in the literature one can find a similar amount of reports suggesting increased numbers of hydrogen bonds with pressure as well as their reduction.[53–56]

Unfortunately, as can be seen in Figure 4, our elevated pressure studies do not reveal a well-separated D-like process. However, before giving some conclusive statements, it is important to note that for ambient pressure data in some cases we also did not record the D-peak (the appearance of the D-relaxation strongly depends on the thermal history of the sample). Additionally, in our loss spectra collected at elevated pressure at frequencies higher than the α-peak appears, the dc conductivity has a strong influence and even after its subtraction from the measured loss it is difficult to state whether the D-process is present or not (Figure 6). Because of this unclear situation, the presence of the D-peak under high pressure still remains an open question. More detailed studies are necessary in the future.

In Figure 7, we present superposed dielectric loss spectra of ibuprofen obtained under different thermodynamic conditions that have approximately the same structural relaxation time τ_α. One can see that the α-relaxation does not change with widely different combinations of p and T; even for very high temperatures and pressures, the shape of the α-peak is the same. This means that the shape of the α-relaxation depends only on the relaxation time τ_α.[57] The invariance of the loss peak with applied pressure and increasing temperature is known in the literature as a temperature−pressure superpositioning (TPS) and was found for many glass-forming liquids, without or with weak hydrogen bonds.[32]

As was reported for *m*-fluoroaniline,[58] glycerol,[59] DPG,[60] and other highly hydrogen-bonded systems, the physical structure of these materials changes at elevated pressure and temperature. It was postulated that breakdown of the TPS is closely related to the modification of the population of the hydrogen bonds under different thermodynamic conditions.[61] In accordance with this finding, the success of TPS for the α-peak in ibuprofen has interesting results, especially because of its strong tendency to create hydrogen-bonding cyclic

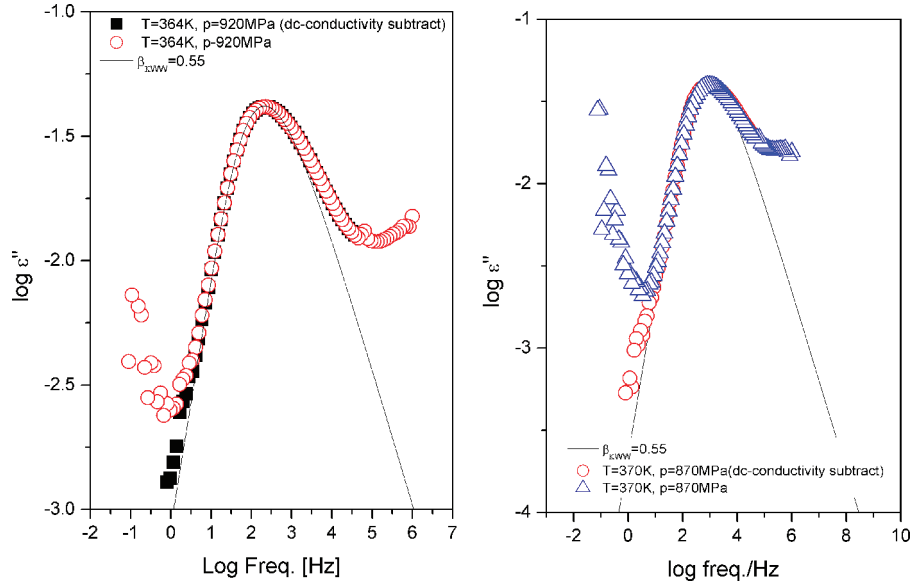

Figure 6. Dielectric loss spectra of ibuprofen collected at $T = 364$ K, $p = 920$ MPa (left panel) and $T = 370$ K, $p = 870$ MPa (right panel). The black solid squares and red open circles are respective spectra after dc-conductivity subtraction.

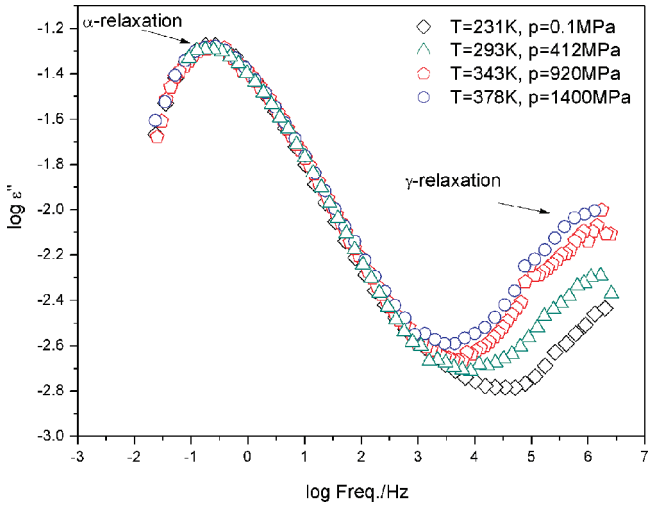

Figure 7. Comparison of the dielectric loss spectra of ibuprofen obtained for different temperature and pressure combinations reported in the figure, with approximately the same structural relaxation time

structures (see ref 39 and references therein). One possible interpretation of this result might be as follows: in a strongly hydrogen-bonded system (like *m*-fluoroaniline or glycerol mentioned above), molecules exhibit a strong tendency to form some more complex hydrogen networks or large clusters, while for ibuprofen the presence of only small hydrogen-bonded aggregates was reported (dimers, trimers). Thus, we may expect that for different pressure and temperature combinations their population even if being modified does not change the structure of a material significantly.

As seen in Figure 7, dielectric loss spectra of ibuprofen collected at higher temperatures and pressures revealed another interesting feature—considerably higher amplitude of the γ-relaxation than that taken at ambient pressure and low temperature. This situation can be related to the compression which each time was carried out at higher temperature, and obviously the amplitude of the γ-relaxation would be higher each time also.

In Figure 8, the structural relaxation times τ_α are displayed as a function of temperature (a) and pressure (b). To describe the temperature and pressure dependences of structural relaxation times, we used the VFT equation and its pressure counterpart[62,63]

$$\log_{10} \tau_\alpha = \log_{10} \tau_a + \frac{D_p P}{P_0 - P} \tag{6}$$

By fitting eq 3 to the isobar at $p = 920$ MPa, we obtained the following sets of parameters: $\log_{10} \tau_\alpha = -18.5 \pm 1.1$ s, $D = 8 \pm 1$, $T_0 = 238 \pm 7$ K. The fitting procedure by eq 6 to the isotherm at $T = 378$ K and $T = 293$ K allowed us to obtain the following values of fitting parameters: $\log_{10} \tau_\alpha = -10.3 \pm 0.4$ s, $D_p = 14.8 \pm 3$, $P_0 = 3400 \pm 300$ MPa and $\log_{10} \tau_\alpha = -7.2 \pm 0.3$ s, $D_p = 17.9 \pm 6$, $P_0 = 1400 \pm 300$ MPa, respectively. Defining a glass transition temperature T_g/glass transition pressure P_g as a temperature (or pressure) at which $\tau_\alpha = 100$ s, we obtained $T_g = 333$ K for the isobaric condition ($p = 920$ MPa) and $P_g = 1550$ MPa for the isothermal condition ($T = 378$ K). Next, these results were used to plot the change in T_g with pressure, as shown in Figure 9. To describe this dependence, we used the empirical relation proposed by Andersson and Andersson[64]

$$T_g(P) = T_g(0)\left(1 + \frac{b}{c}P\right)^{1/b} \tag{7}$$

with $T_g(P{=}0) = 225 \pm 1$ K, $b = 3.2 \pm 0.1$, and $c = 1153 \pm 48$ MPa. Thus, in the limit of zero pressure, dT_g/dP is equal to 0.195 ± 0.009 K/MPa. The value of dT_g/dP found for ibuprofen is much higher than those reported previously for strongly hydrogen-bonded systems like glycerol (0.04 K/MPa[65]), sorbitol (0.043 K/MPa[66]), or propylene glycol (0.037 K/MPa[67]) but comparable to those of van der Waals liquids.[41] Interestingly, it is similar to that for salol[68] ($dT_g/dP = 0.204 \pm 0.01$ K/MPa), the glass former with roughly the same molecular weight. What is more, because of the presence of the hydroxyl and carbonyl moieties in salol, its possibility for hydrogen-bonded formation is also suggested. We would like to use the similarity between

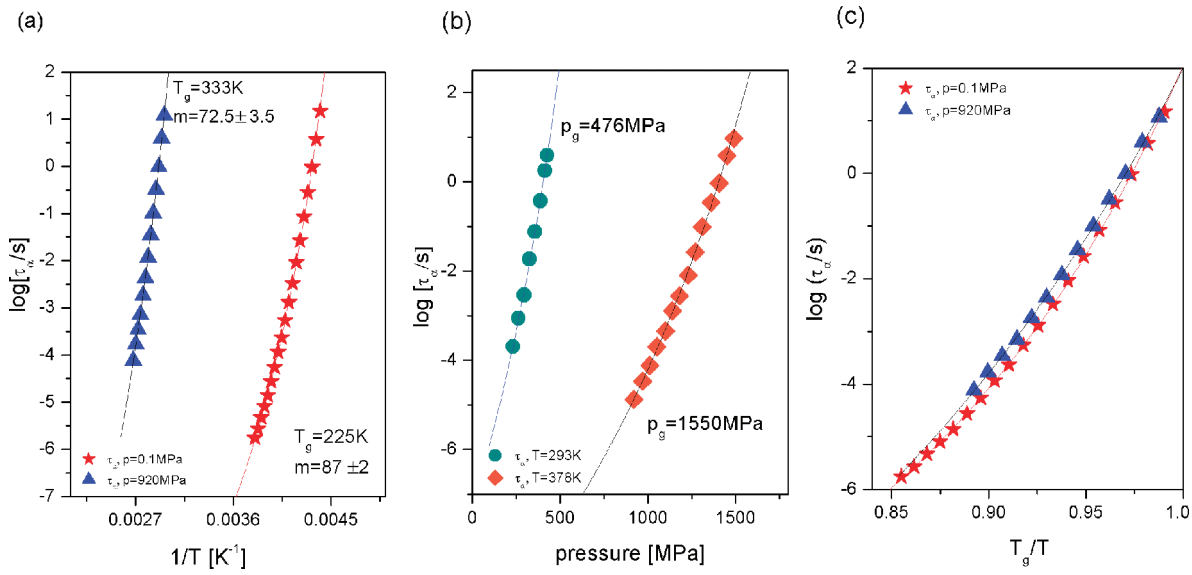

Figure 8. Temperature (a) and pressure (b) dependences of structural relaxation times obtained during isobaric and isothermal measurements. The solid lines represent fits to the temperature VFT equation and its pressure counterpart. (c) Schematic diagram for the fragility (Angell plot), where the logarithm of structural relaxation time α was plotted against the T_g-scaled reciprocal temperature.

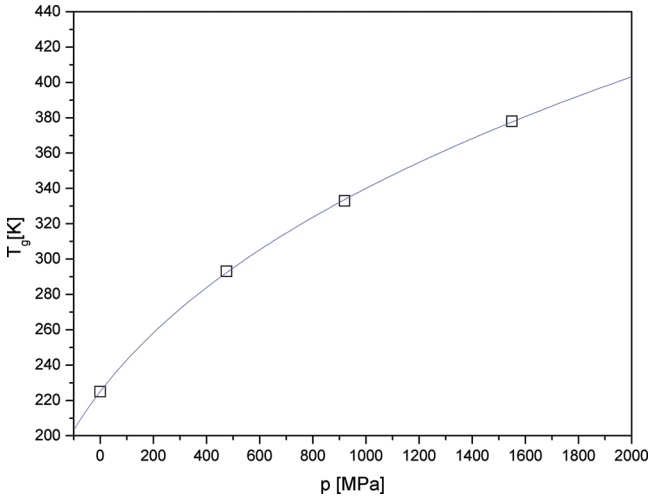

Figure 9. Pressure dependence of the glass transition temperature. The solid line represents the fit to the Andersson and Andersson equation.

those compounds in the next section to demonstrate an average change in density of supercooled liquid under compression.

From the VFT fits to the temperature dependence of α-relaxation times at pressure $p = 920$ MPa, we also calculated the fragility index in accordance with eq 4. We found that at this pressure the steepness index is equal to $m = 72.5 \pm 3.5$, which is a clear sign that fragility decreases with compression (note that $m = 87 \pm 2$ at ambient pressure). This was also illustrated on the so-called "Angell plot" (Figure 8c).

Very similar behaviors have been reported previously for other APIs like indomethacin[32] or verapamil hydrochloride[22] and many more nonpharmaceutical systems belonging to the van der Waals class of liquids.[41] Interestingly, in the case of strongly hydrogen-bonded systems, a completely opposite behavior is frequently observed, i.e., the increase of fragility m with pressure, which probably results from complete or nearly complete reduction of hydrogen bonds with applying pressure.[60,69]

The drop of fragility with compression observed for ibuprofen agrees with prediction of the TOP model. The reduction of fragility with pressure implies that the liquid becomes stronger/less fragile (or more frustrated in accordance with the TOP model) and consequently should be more stable against crystallization than the fragile one (less frustrated). The reduction of the fragility of liquid due to its compression seems to have very important implications in many fields of science, especially pharmaceutical industry, to extend the long-term stability of glassy drugs. However, in the particular case of ibuprofen, it is impossible to use under ambient conditions a glass produced at high pressure, since the glass transition temperature of ibuprofen at atmospheric pressure lies far below room temperature.

At the end of this section, we would like to make some comments on the relationship between the density of glass and its stability against crystallization. As it was shown for indomethacin,[25] the increase in the density of glass, roughly by about 2%, results in significant improvement of its stability. On the molecular level, one can imagine that high density glass has molecules which are packed more densely compared to "ordinary" glasses and obviously has less free volume available. Of course, it is also reasonable to suppose that a specific volume of denser glass would be lower than that for a glass obtained by supercooling melt. Moreover, the difference in specific volumes, ΔV, between a glass and crystal ($\Delta V = V_{glass} - V_{cryst}$) for a denser system should also be lower. Intriguingly, very recently, Tanaka has showed that, for materials with large ΔV, the crystal growth rate below T_g is faster than that for others with smaller ΔV.[70] He argued that, for a material with larger ΔV, the volume contraction upon crystallization provides a crystal−glass interface with large excess free volume, which results in increase of mobility at the growth front and results in enhanced crystal growth in the glassy state.[70] It seems that his finding might be one of the possible explanations for why denser glasses are more stable against crystallization.

3.3. Crystallization Kinetics. Crystallization kinetics can be studied by several techniques like differential scanning calorimetry (DSC), differential thermal analysis (DTA), or X-ray diffraction (XRD). However, herein we have employed dielectric spectroscopy (DS). Through a reduction of the dielectric strength $\Delta\varepsilon$ of the structural relaxation process with crystallization progress, this method enabled us to monitor crystallization directly at real-time of measurements. It is worth noting that the drop of dielectric strength $\Delta\varepsilon$ with time evolution is caused

by reduction of the number n of reorientating dipoles with crystallization progress ($\Delta\varepsilon \propto n\mu^2$).

Very recently, Dudognon and co-workers have prepared DSC measurements of the nucleation and crystal growth rate of racemic ibuprofen at ambient pressure.[42] Their studies revealed that between 233 and 263 K the most favorable nucleation and crystal growth rate occur. On the basis of their finding and our own time-dependent measurements of induction time t_0 at several temperatures in this temperature region, we have selected $T = 255$ K for which t_0 at ambient pressure was reasonable short (about 1 h).

For ibuprofen, we have studied the crystallization kinetics at three different thermodynamical conditions: sample 1 crystallized at $T_1 = 255$ K and $p_1 = 0.1$ MPa, sample 2 at $T_2 = 343$ K and $p_2 = 550$ MPa, and sample 3 at $T_3 = 383$ K and $p_3 = 920$ MPa. The conditions mentioned above were carefully selected, so that their structural relaxation times were approximately the same ($\tau_\alpha \approx 1 \times 10^{-5}$ s). The purpose of this research was to find if there is any difference in the crystallization behavior under ambient and high pressure. During our measurements of dielectric response function at given sets of pressure and temperature combinations after a waiting time t_0 in which the changes in spectra were not observed, the onset of crystallization occurred, resulting in a dramatic change in their response. This situation is clearly seen in Figure 10, where the evolution of the real (ε') and imaginary (ε'') parts of complex dielectric permittivity for all studied samples are presented. During crystallization progress, the intensity of the α-relaxation peak gradually decreases. In the real part of the complex dielectric permittivity, this situation is reflected by a decrease of static permittivity increment. However, at the end of the crystallization time, the effect of electrode polarization shows up in addition to dc conductivity, which results in difficulty monitoring the α-peak at the final stage of crystallization.

It is worth noting that, even in advanced crystallization progress, after significant depletion of the loss peaks, we did not observe additional relaxation processes, indicating other mobility.

In order to evaluate the changes in the loss peaks during crystallization, we have fitted experimental data by the Havriliak−Negami function (HN)[71]

$$\varepsilon^*(f) = \varepsilon' + \frac{\Delta\varepsilon}{[1 + (i\omega\tau_{HN})^{\alpha_{HN}}]^{\beta_{HN}}} \qquad (8)$$

where τ_{HN} denotes a characteristic relaxation time and α_{HN} and β_{HN} are parameters that characterize the shape of the dielectric loss curve. Representative values of the shape parameters α_{HN} and β_{HN} determined from fitting analysis for the studied samples are given in Table 1. Interestingly, the shape of the initial loss peaks for each sample differs. The broadening of the structural relaxation peak observed for samples 2 and 3 when compared to the sample crystallized at low temperature and ambient pressure (sample 1) can be explained by the strong influence of the γ-relaxation process. This process, despite its insensitivity to pressure, at higher temperatures might have similar or even greater amplitude than the α-peak. Because of that reason, it may result in enormous broadening of the structural relaxation peak, especially the high frequency flank of the loss peak. In early stages of crystallization, we observed that shapes of the α-relaxation peaks practically do not change. A very similar behavior is reported for Paracetamol[72] or SSR drug.[14]

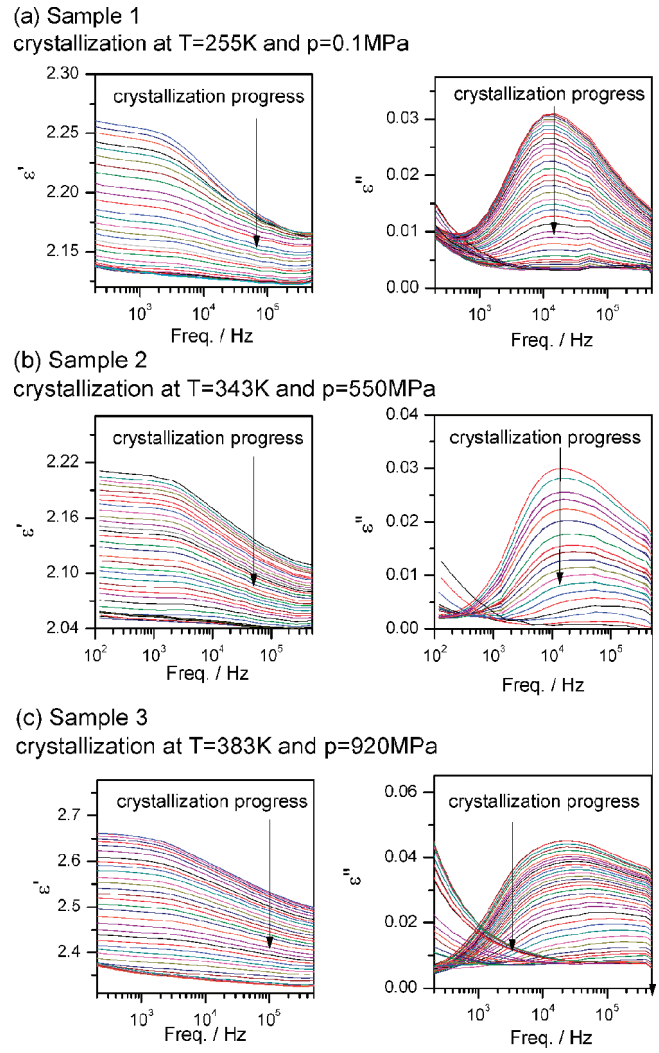

Figure 10. Spectra of the real (ε') and imaginary (ε'') part of complex dielectric permittivity in the frequency domain during crystallization of ibuprofen at (a) $T = 255$ K and $p = 0.1$ MPa, (b) $T = 343$ K and $p = 550$ MPa, and (c) $T = 383$ K and $p = 920$ MPa.

TABLE 1: Representative Values of the Shape Parameters and Structural Relaxation Times in the Initial Stages of Crystallization for All Studied Samples of Ibuprofen

	crystallization progress (s)	α_{HN}	β_{HN}	τ_α (s)
sample 1	0	0.92	0.34	1.1×10^{-5}
	10800	0.93	0.34	1.1×10^{-5}
	20400	0.92	0.33	1.1×10^{-5}
	33000	0.91	0.32	9.9×10^{-6}
	50400	0.90	0.30	7.2×10^{-6}
sample 2	0	0.92	0.26	1.1×10^{-5}
	31800	0.93	0.26	1.1×10^{-5}
	60000	0.92	0.27	1×10^{-5}
	100200	0.91	0.24	9.4×10^{-6}
	144600	0.9	0.23	7.4×10^{-6}
sample 3	0	0.88	0.22	9×10^{-6}
	20400	0.88	0.19	8.7×10^{-6}
	50400	0.87	0.18	7.8×10^{-6}
	126000	0.85	0.16	5.6×10^{-6}
	160800	0.83	0.13	4.5×10^{-6}

For all three samples, the α-relaxation time τ_α was defined as

$$\tau_\alpha = \frac{1}{2\pi f_{max}} \qquad (9)$$

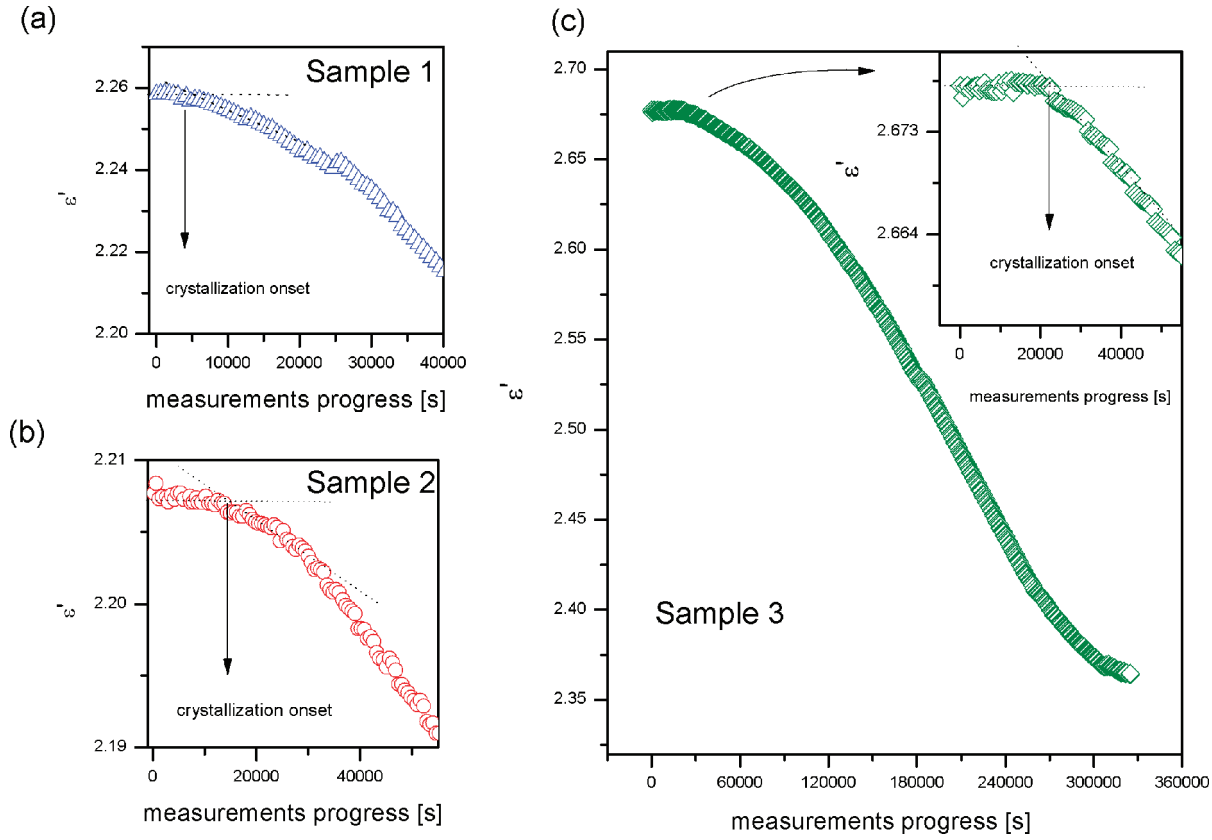

Figure 11. Panels a and b and inset c present the evolution of the dielectric constant of α-relaxation, at the low frequency region, during the first stage of measurements, for samples 1, 2, and 3, respectively. During measurements at given sets of pressure and temperature combinations after a waiting time in which the changes in spectra were not observed, the dielectric constant of the α-process starts to decrease. The main figure in panel c presents the evolution of the dielectric constant of structural relaxation throughout the whole measurement time.

where f_{max} is the frequency of the maximum peak position. The variation of structural relaxation times during crystallization can also be found in Table 1. As can be seen, the position of the α-maxima during crystallization evaluate toward faster relaxation times. Time evolution of the structural relaxation peak during crystallization is a frequently observed phenomenon.[73,74]

The crystallization kinetics of ibuprofen was studied in the real part of the complex dielectric permittivity. Since the position of the structural relaxation peak during crystallization slowly moves toward higher frequencies, the $\varepsilon'(t)$ dependences used in further analysis were recorded from the low frequency region (between 200 and 1400 Hz), where they are practically frequency independent. Unfortunately, due to the large contribution of electrode polarization at the final stages of crystallization, we were unable to monitor complete reduction of static permittivity increment to the value, indicating 100% crystallinity.

Next, we have measured the induction time of crystallization t_0 for the studied samples. It is important to note here that since the structural relaxation times and also viscosities were the same one should expect very similar onsets of crystallization if molecular mobility related to the α-process is responsible for crystallization. However, our observation clearly shows that the induction time of crystallization (t_0, defined as a time where the dielectric constant starts to decrease) significantly increases for samples 2 and 3 (see Figure 11). In these cases, the induction times were equal to $t_0 \cong 4$ h for sample 2 and $t_0 \cong 5.6$ h for sample 3, while for sample 1 (crystallizes at ambient pressure) this time took only $t_0 \cong 1.2$ h. This is a clear indication that mobility does not alone govern the crystallization.

To monitor the crystallization kinetics, we have used the normalized dielectric constant given by[75]

$$\varepsilon'_N(t) = \frac{\varepsilon'(0) - \varepsilon'(t)}{\varepsilon'(0) - \varepsilon'(\infty)} \tag{10}$$

where $\varepsilon'(0)$ is the dielectric constant at the beginning of crystallization, $\varepsilon'(\infty)$ is the long time limiting value of the dielectric constant, and $\varepsilon'(t)$ is the value at time t. Normalized curves plotted versus time are presented in Figure 12a. As expected, the $\varepsilon'_N(t)$ curve shifts to a longer time as the crystallization temperature and pressure increase.

We have also calculated the crystallization half-time, as a time at which the crystallinity reached 50% of the maximum crystallinity. We obtained $t_{1/2} = 12.2$ h for sample 1, $t_{1/2} = 35.7$ h for sample 2, and $t_{1/2} = 49$ h for sample 3. These results indicate that when crystallization is carried out at high pressure the overall crystallization time is extended.

To describe the time dependence of the normalized dielectric constant $\varepsilon'_N(t)$, one can use the Avrami equation[76,77]

$$\varepsilon'_N(t) = 1 - \exp[-kt^n] \tag{11}$$

where$k$ is the rate constant and n is the Avrami exponent. The value of n depends on the crystal morphology and crystallization mechanism.[78]

The usual way to obtain Avrami parameters is to plot $\ln(-\ln(1 - \varepsilon'_N))$ versus $\ln(t)$. A straight line is expected having n as the slope and $-\ln k$ as the intercept with y-axis. The Avrami plots

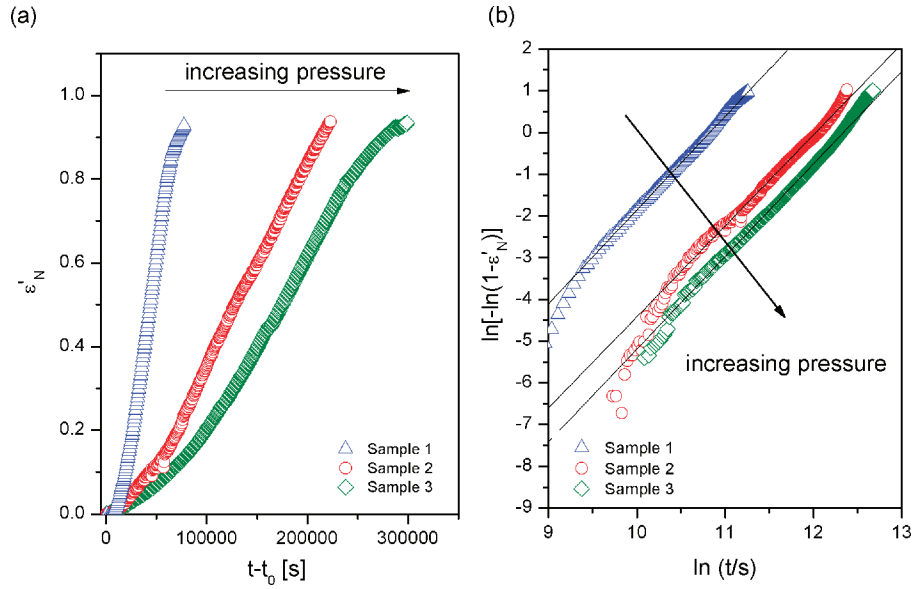

Figure 12. (a) Normalized dielectric constant ε'_N as a function of crystallization time for crystallization carried out at $p = 0.1$ MPa and $T = 255$ K (sample 1), $p = 550$ MPa and $T = 343$ K (sample 2), and $p = 920$ MPa and $T = 383$ K (sample 3). (b) Avrami plot of the normalized dielectric constant ε'_N for ibuprofen and different crystallization temperatures and pressures. The solid lines represent fits to the Avrami equation. Blue triangles are for sample 1, red circles for sample 2, and green squares for sample 3.

TABLE 2: Kinetic Parameters Obtained Using the Avramov and Avrami Approaches for Ibuprofen

	Avrami		Avramov				
material	n	$-\ln k$	n	τ_{cry} (h)	induction time t_0 (h)	half time $t_{1/2}$ (h)	rate constant k (s^{-n}) (calculated from eq 15)
ibuprofen sample 1 ($p = 0.1$ MPa, $T = 255$ K)	2.3	−24.7	2.2	13	1.2	12.2	1.7×10^{-11}
ibuprofen sample 2 ($p = 550$ MPa, $T = 343$ K)	2.2	−26.3	2.2	38.5	4	35.7	1.5×10^{-12}
ibuprofen sample 3 ($p = 920$ MPa, $T = 383$ K)	2.2	−27.4	2.3	52	5.5	49	7.3×10^{-13}

for ibuprofen are shown in Figure 12b. The values of fitting parameters are given in Table 2, albeit a clear deviation from linearity is observed. A very similar situation was reported by Avramov.[79] A few years ago, he pointed out that in double logarithmic scale the method proposed by Avrami exaggerates the role of initial states (small value of ε'_N) and final stages (the value of ε'_N close to 1) of the crystallization process.

In order to avoid any errors while determining the values of n and k parameters, instead of the Avrami equation, one can use the Avramov approach. In this case, the value of ε'_N is plotted versus $\ln(t - t_0)$. To obtain n and the characteristic time of the crystallization process τ_{cry}, the first derivate of ε'_N with respect to $\ln(t - t_0)$ has to be plotted in the same graph with ε'_N vs $\ln(t - t_0)$ dependence, as seen in Figure 13. The value of n can be determined as

$$n = \frac{(\varepsilon'_N)'_{max}}{0.368} \tag{12}$$

where $(\varepsilon'_N)'_{max}$ is the maximum first derivative of the normalized dielectric constant.

The value of n can be calculated also from the following equation

$$n = \frac{e}{\ln t_2 - \ln t_1} \tag{13}$$

where $\ln t_2$ and $\ln t_1$ are the intersection between the tangent to ε'_N in $(\varepsilon'_N)'_{max}$ with $\varepsilon'_N = 0$ and $\varepsilon'_N = 1$, respectively. The value of the Avrami parameter n and characteristic time for the crystallization process, τ_{cry}, obtained using this Avramov approach are given in Table 2. Since a detailed description of this method is beyond the scope of this paper, for more information, the reader is referred to the original Avramov paper[79] as well as the work of S. Napolitano and M. Wübbenhorst.[80] It is very remarkable that the values of the parameter "n" obtained for the samples studied herein which crystallize under completely different thermodynamic conditions are practically the same. This is a clear sign of the nonchanging shape of growing crystals. The value of n close to 2 indicates athermal nucleation followed by two-dimensional crystal growth. In this case, we may expect that the crystals grow as rods. However, their nonintegral values may also suggest mixed growth and surface nucleation, and/or two-step crystallization.

Next, to calculate the rate constant k, we have transformed the following relation:

$$t_{1/2} = \left(\frac{\ln 2}{k}\right)^{1/n} \tag{15}$$

We get that the constant rate for a sample crystallized at ambient pressure is equal to $k = 1.7 \times 10^{-11}\ s^{-n}$, while for samples 2 and 3 $k = 1.5 \times 10^{-12}\ s^{-n}$ and $k = 7.3 \times 10^{-13}\ s^{-n}$, respectively. These values of rate constants imply that the crystallization rate decreases with compression.

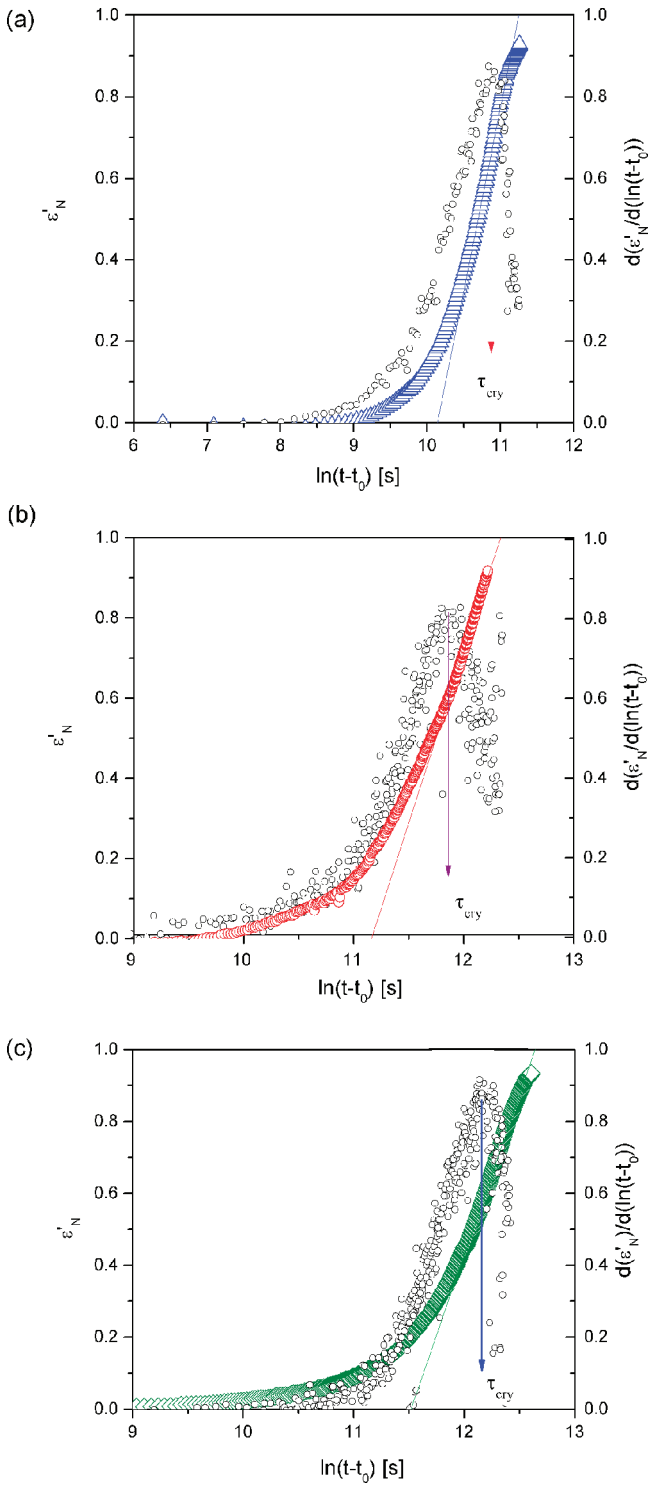

Figure 13. Dependence of normalized dielectric constant ε'_N and its first derivative versus logarithm of the time, analyzed in accordance with the Avramov method: (a) crystallization at $T = 255$ K and $p = 0.1$ MPa (sample 1); (b) crystallization at $T = 343$ K and $p = 550$ MPa (sample 2); (c) crystallization at $T = 383$ K and $p = 920$ MPa (sample 3).

In summary, the results presented in this section clearly show that for a crystallization at high pressure (samples 2 and 3) the induction time as well at the overall crystallization time takes definitely more time than for a sample crystallized at normal pressure (sample 1). Except for slowing down of the crystallization progress, as happened in our case, the pressure can also suppress the crystallization completely, as shown for TPP.[34] On the other hand, one should still remember that in the literature one can find lots of examples which demonstrate that the pressure can catalyze crystallization.[81,82] However, as was shown more than 10 years ago by Gutzow et al., for most liquids, pressure does not increase the maximal nucleation and crystal growth rate but rather shifts it to higher temperatures.[83] On the basis of his point of view on the thermodynamic and kinetic consequences of hydrostatic pressure on melt crystallization, elongated induction time and overall crystallization time for our samples 2 and 3 can be explained as follows: The pressure moved the nucleation and crystal growth process to higher temperatures. In this case, T_{max}, that is, the temperature where the maximum of crystal nucleation rate occurred, is situated also at a much higher temperature, where obviously the melt has a lower viscosity. In addition, the decrease of crystal growth rate at T_{max} is expected. Since the pressure shifts only T_{max} to the lower viscosity region, it does not affect the viscosities of samples 2 and 3, which are the same as that crystallized at ambient pressure. As a result of pressure, ibuprofen crystallized at high temperature and high pressure is far away from maximum where its optional crystallization rate occurred. Thus, the induction time t_0 and crystallization half-time $t_{1/2}$ for these samples are significantly extended. The explained above scenario is the most probable one.

Moreover, it is highly expedient to point out the difference in the densities of both samples. We suppose sample 3 would be denser than sample 1. While we were not able to experimentally measure the density changes for pressurized liquid ibuprofen, to outline the expected differences in densities between samples kept under different thermodynamic conditions (T_1, p_1) and (T_3, p_3), we made use of the PVT data of salol.[84] Here, we based on similarities between both systems, but it is given only as an approximation and the obtained results cannot be taken as highly accurate.

It is well-known that the volume for any combination of temperature and pressure can be calculated from the Tait equation.[85,86] The fitting procedure allowed us to obtain $V_1 = 0.8098$ cm^3/g at $T_1 = 255$ K and $p_1 = 0.1$ MPa and $V_3 = 0.7288$ cm^3/g at $T_3 = 383$ K and $p_3 = 920$ MPa. Hence, for the liquid state of our pressurized sample 3, we expect about 10% increase of density.

Finally, we would like to also verify whether the crystallization carried out at high pressure may lead to any new polymorphic form of ibuprofen. Especially that from the literature, it is well-known that pressure may affect polymorphic transformations like what happened for indomethacin.[87] If really crystallization under high pressure and temperature conditions leads to different crystalline phases, it could be very interesting for the pharmaceutical industry. It is worth mentioning that physical stability, solubility, or bioavailability can differ significantly for various polymorphic forms of drugs.[88,89] In accordance with results presented in Cambridge Crystalline Data Centre (CCDC),[90] the racemic (*R*/*S*) ibuprofen crystals are orthorhombic, with a non-centrosymmetric space group $Pca2_1$, while the pharmaceutically active *S*-enantiomer is monoclinic, with the space group $P2_1$. It is also worth noting that racemic ibuprofen crystallized using various methods (like cooling hot solution, solvent exchange method, and precipitation from solution) has different crystal habits,[91,92] which results for example in the mechanical properties of this drug. It is also interesting to note that the techniques mentioned above do not lead to any polymorphic form.[91] However, as shown by E. Dudognon and co-workers,[42] ibuprofen revealed a solid state polymorphism. The new crystalline form can be obtain by cold-

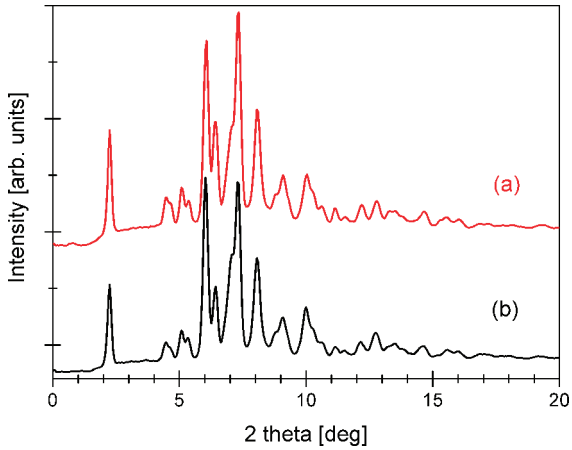

Figure 14. X-ray powder diffraction patterns taken at ambient conditions of conventional crystalline ibuprofen (a) and crystal obtained under high pressure—sample 2 (b).

crystallization at 255 K and ambient pressure after earlier annealing (1 h) of the sample at a temperature 60 K lower than its T_g. It is worth pointing out that new crystal formation is highly metastable and melts at room temperature (almost 60 K below T_m of the conventional phase).

The X-ray diffraction measurements were performed on the selected sample (sample 2). Unfortunately, due to technical reasons, we were not able to perform it directly under the pressure and temperature conditions in which that sample crystallized. Thus, the X-ray studies were carried out under ambient conditions, after slow decompression proceeded by cooling down sample 2 to room temperature. The X-ray powder diffraction patterns of conventional crystalline ibuprofen (taken as a reference) and crystal obtained under high pressure were taken at room temperature and are displayed in Figure 14a and b, respectively. One can see that the peak positions as well as their intensities are practically the same. This result indicates that the crystalline structures of sample 2 and conventional ibuprofen at room temperature are the same, with no signs of polymorphism. However, certainty that sample 2 does not crystallize to another form would ensure only X-ray studies carried out at $p = 550$ MPa and $T = 343$ K. Here, we must also reconsider the fact than if the new polymorphic form of ibuprofen can be obtained by crystallization at high pressure it might be highly metastable (like that found by Dudognon and co-workers[42]) and during decompression and decreasing temperature to standard conditions it would revert to a more stable initial form. Thus, some more detailed studies on that aspect should be performed in the future.

4. Summary

The following conclusion can be drawn from our studies of dielectric relaxation and crystallization kinetics of ibuprofen under ambient and elevated pressure:

(i) We found good agreement between our data taken at ambient pressure and that published earlier in the literature. However, we noticed that appearance of the D-process, associated with hydrogen-bonded cyclic structures formed by ibuprofen molecules, is strongly dependent on the thermal history of the sample.

(ii) In dielectric loss spectra taken at elevated pressure expect D-relaxation, we observed the same relaxation process as for ambient pressure studies. The γ-process, insensitive to pressure change, was classified as a non-JG. The β-relaxation, submerged above the glass transition temperature, is clearly visible in spectra below the T_g. The increase of activation energy of the β-process for the isobar taken at high pressure ($p = 1750$ MPa) indicates that this relaxation is sensitive to pressure, i.e., density change. By comparing spectra taken at different pressure and temperature combinations but having exactly the same α-relaxation time, we found that the loss peak obeys the pressure−temperature superpositioning. This result suggests that even if a population of small hydrogen-bonded ibuprofen aggregates is being modified under pressure it does not significantly change the structure of a material. For ibuprofen, the zero pressure limiting value of dT_g/dP is equal to 0.195 $\pm$ 0.009 K/MPa. It is of course a rather high value compared to strongly hydrogen-bonded systems but similar to that previously found for salol ($dT_g/dP = 0.204 \pm 0.01$ K/MPa), a small molecule with hydrogen-bonding possibilities. We also found that, with compression, the value of the fragility index decreases from $m = 87 \pm 2$ at atmospheric pressure to $m = 72.5 \pm 3.5$ at high pressure ($p = 920$ MPa). The drop of fragility observed in our experiment is in accord with the prediction given by the TOP model. Because of that reason, we argue that glassy ibuprofen, prepared by compression, should be more stable against crystallization than one obtained in the ordinary way (supercooling melt). This fact was explained on the basis of Tanaka's approach.

(iii) The overall crystallization kinetics has been studied for three samples of ibuprofen, with the same structural relaxation time but for different pressure and temperature combinations. Our measurements revealed significant extension of induction time as well as the overall crystallization time for ibuprofen crystallized under high pressure compared to that crystallized at ambient pressure. This can be explained due to the shift of the optimal nucleation and crystal growth process to higher temperatures with pressure. We also pointed out the difference between the densities of samples 1 and 3 (roughly about 10% in the supercooled state) upon the same molecular mobility. Interestingly, the value of the Avrami parameter n was recorded to be practically the same for ibuprofen crystallized under ambient and high pressure, which suggests nonchanging shape of growing crystals.

(iv) Our additional X-ray diffraction studies carried out under ambient conditions indicate that the crystalline structures of sample 2 and conventional ibuprofen are the same, with no signs of polymorphism.

Acknowledgment. The authors (K.A., Z.W., K.K., and M.P.) are deeply thankful for the financial support within the framework of the project entitled "From Study of Molecular Dynamics in Amorphous Medicines at Ambient and Elevated Pressure to Novel Applications in Pharmacy", which is operated within the Foundation for Polish Science Team Programme cofinanced by the EU European Regional Development Fund. K.A. and Z.W. would like to thank A. Szulc for technical assistance during high pressure measurements. S.P. acknowledges financial assistance from FNP HOMING program (2008) supported by the European Economic Area Financial Mechanism.

References and Notes

(1) www.drugbank.ca.

(2) Kasim, N. A.; Whitehouse, M.; Ramachandran, C.; Bermejo, M.; Lennernäs, H.; Hussain, A. S.; Junginger, H. E.; Stavchansky, S. A.; Midha, K. K.; Shah, V. P.; Amidon, G. L. *Mol. Pharm.* **2004**, *1* (1), 85–96.

(3) Lindenberg, M.; Kopp, S.; Dressman, J. B. *Eur. J. Pharm. Biopharm.* **2004**, *58* (2), 265–278.
(4) Hancock, B. C.; Parks, M. *Pharm. Res.* **2000**, *17* (4), 397–404.
(5) Gupta, P.; Chawla, G.; Bansal, A. K. *Mol. Pharm.* **2004**, *1* (6), 406–413.
(6) Craig, D. Q. M.; Royall, P. G.; Kett, V. L.; Hoptopn, M. L. *Int. J. Pharm.* **1999**, *179* (2), 179–207.
(7) Kaminski, K.; Kaminska, E.; Adrjanowicz, K.; Grzybowiska, K.; Wlodarczyk, P.; Paluch, M.; Burian, A.; Ziolo, J.; Lepek, P.; Mazgalski, J.; Sawicki, W. *J. Pharm. Sci.* **2010**, *99* (1), 94–106.
(8) Gupta, P.; Bansal, A. K. *AAPS PharmSciTech* **2005**, *6* (2), 223–230.
(9) Aso, Y.; Yoshioka, S.; Kojima, S. *J. Pharm. Sci.* **2000**, *89* (3), 408–416.
(10) Yoshioka, M.; Hancock, B. C.; Zografi, G. *J. Pharm. Sci.* **1994**, *83* (12), 1700–1705.
(11) Hancock, B. C.; Shamblin, S. L.; Zografi, G. *Pharm. Res.* **1995**, *12* (6), 799–806.
(12) Andronis, V.; Zografi, G. *Pharm. Res.* **1998**, *15* (6), 835–842.
(13) Yoshioka, S.; Aso, Y. *Pharm. Res.* **2005**, *22* (8), 1358–1364.
(14) Alie, J.; Menegotto, J.; Cardon, P.; Duplaa, H.; Caron, A.; Lacabanne, C.; Bauer, M. *J. Pharm. Sci.* **2004**, *93* (1), 218–233.
(15) Hikima, T.; Hanaya, T.; Oguni, M. *J. Mol. Struct.* **1999**, *479* (Issues 2−3), 245–250.
(16) Hikima, T.; Hanaya, T.; Oguni, M. *Bull. Chem. Soc. Jpn.* **1996**, *69* (7), 1863–1868.
(17) Hikima, T.; Hanaya, T.; Oguni, M. *J. Non-Cryst. Solids* **1998**, *235*−*237*, 539–547.
(18) Okamoto, N.; Oguni, M.; Sagawa, Y. *J. Phys.: Condens. Matter* **1997**, *9*, 9187.
(19) Medeiros, A. F. D.; Santos, A. F. O.; de Souza, F. S.; Procópio, J. V. V.; Pinto, M. F.; Macêdo, R. O. *J. Therm. Anal. Calorim.* **2007**, *88* (2), 311–315.
(20) Crowley, K. J.; Zografi, G. *J. Pharm. Sci.* **2002**, *91* (2), 492–507.
(21) Hedoux, A.; Guinet, Y.; Capet, F.; Paccou, L.; Decamps, M. *Phys. Rev. B* **2008**, *77* (9), 094205.
(22) Wojnarowska, Z.; Paluch, M.; Grzybowski, A.; Adrjanowicz, K.; Grzybowska, K.; Kaminski, K.; Wlodarczyk, P.; Pionteck, J. *J. Chem. Phys.* **2009**, *131* (10), 104505.
(23) Dawsona, K. J.; Kearnsa, K. L.; Lian, Yub; Steffenc, W.; Ediger, M. D. *Proc. Natl. Acad. Sci. U.S.A.* **2009**, *106* (36), 15165–15170.
(24) Surana, R.; Pyne, A.; Suryanarayanan, R. *Pharm. Res.* **2004**, *21* (5), 867–874.
(25) Kearns, K. L.; Swallen, S. F.; Ediger, M. D.; Wub, Tian; Yu, Lian *J. Chem. Phys.* **2007**, *127*, 154702.
(26) Fukuoka, E.; Markita, M.; Yamamura, S. *Chem. Pharm. Bull.* **1986**, *34* (10), 4314–4321.
(27) Bates, S.; Zografi, G.; Engers, D.; Morris, K.; Crowley, K.; Newman, A. *Pharm. Res.* **2006**, *23* (10), 2333–2349.
(28) Kearns, K. L.; Swallen, S. F.; Ediger, M. D.; Ye, Sun; Lian, Yu *J. Phys. Chem. B* **2009**, *113* (6), 1579–1586.
(29) Dawson, K. J.; Kearns, K. L.; Sacchetti, M.; Zografi, G.; Ediger, M. D. *J. Phys. Chem. B* **2009**, *113* (8), 2422–2427.
(30) Paluch, M.; Pawlus, S.; Hensel-Bielowka, S.; Kaminski, K.; Psurek, T.; Rzoska, S. J.; Ziolo, J.; Roland, C. M. *Phys. Rev. B* **2005**, *72* (22), 224205.
(31) Kaminski, K.; Kaminska, E.; Hensel-Bielowka, S.; Pawlus, S.; Paluch, M.; Ziolo, J. *J. Chem. Phys.* **2008**, *129* (8), 084501.
(32) Wojnarowska, Z.; Adrjanowicz, K.; Wlodarczyk, P.; Kaminska, E.; Kaminski, E.; Grzybowska, K.; Wrzalik, R.; Paluch, M.; Ngai, K. L. *J. Phys. Chem. B* **2009**, *113* (37), 12536–12545.
(33) Sharifi, S.; Prevosto, D.; Capaccioli, S.; Lucchesi, M.; Paluch, M. *J. Non-Cryst. Solids* **2007**, *353* (47−51), 4313–4317.
(34) Mierzwa, M.; Paluch, M.; Rzoska, S. J.; Ziolo, J. *J. Phys. Chem. B* **2008**, *112* (34), 10383–10385.
(35) Tanaka, H. *J. Chem. Phys.* **1999**, *111* (7), 3175–3183.
(36) Tanaka, H. *J. Chem. Phys.* **1999**, *111* (7), 3163–3175.
(37) Tanaka, H. *J. Non-Cryst. Solids* **2005**, *351* (43−45), 3371–3384.
(38) Johari, G. P.; Kim, S.; Shanker, R. M. *J. Pharm. Sci.* **2007**, *96* (49−51), 1159–1175.
(39) Brás, A. R.; Noronha, J. P.; Antunes, A. M.; Cardoso, M. M.; Schönhals, A.; Affouard, F.; Dionísio, M.; Correia, N. T. *J. Phys. Chem. B* **2008**, *112* (35), 11087–11099.
(40) Lerdkanchanaporn, S.; Dollimore, D. *J. Therm. Anal.* **1997**, *49* (2), 879–886.
(41) Roland, C. M.; Hensel-Bielowka, S.; Paluch, M.; Casalini, R. *Rep. Prog. Phys.* **2005**, *68* (6), 1405–1478.
(42) Dudognon, E.; Danède, F.; Decamps, M.; Correia, N. T. *Pharm. Res.* **2008**, *25* (12), 2853–2858.
(43) Wang, L. M.; Richert, R. *J. Phys. Chem. B* **2005**, *109* (22), 11091–11094.
(44) Wang, L. M.; Richert, R. *J. Chem. Phys.* **2004**, *121* (22), 11170–11176.
(45) Jakobsen, B.; Maggi, C.; Christensen, T.; Dyre, J. C. *J. Chem. Phys.* **2008**, *129* (18), 184502.
(46) Kohlrausch, R. *Ann. Phys* **1847**, *72*, 393. Williams, G.; Watts, D. C. *Trans. Faraday Soc.* **1970**, *66*, 80–85.
(47) Vogel, H. *Phys. Z.* **1921**, *22*, 645–646. Fulcher, G. *J. Am. Ceram. Soc.* **1925**, *8* (6), 339–355. Tammann, G.; Hesse, W. *Z. Anorg. Allg. Chem.* **1926**, *156* (1), 245–257.
(48) Ngai, K. L.; Rendell, R. W. In *Supercooled Liquids, Advances and Novel Applications*; Fourkas, J. T., Kivelson, D., Mohanty, U., Nelson, K., Eds.; ACS Symposium Series Vol. 676; American Chemical Society: Washington, DC, 1997; Chapter 4, p 45.
(49) Ngai, K. L.; Casalini, R.; Cappacioli, S.; Paluch, M.; Roland, C. M. Dispersion of the Structural Relaxation and the Vitrification of Liquids. In *Volume in monograph Fractals, diffusion and Relaxation in Disordered Complex Systems, Advances in Chemical Physics*; Kalmykov, Y. P., Coffey, W. T., Rice, S. A., Eds.; Wiley: New York, 2006; Vol. 133, pp 79−138.
(50) Popa, M. I.; Gabriela, Lisa; Aelenei, N. *Polym. Bull.* **2008**, *61*, 481–490.
(51) Lerdkanchanaporn, S. *Thermochim. Acta* **1999**, *340*−*341*, 131–138.
(52) Ngai, K. L.; Paluch, M. *J. Chem. Phys.* **2004**, *120* (2), 857–873.
(53) Freeman, B. D.; Bokobza, L.; Sergot, P.; Monnerie, L.; De-Schryver, F. C. *Macromolecules* **1990**, *23* (9), 2566–2573.
(54) Cook, R. E.; King, H. E.; Peiffer, D. G. *Phys. Rev. Lett.* **1992**, *69* (21), 3072–3075.
(55) Prevosto, D.; Capaccioli, S.; Lucchesi, M.; Rolla, P. A.; Paluch, M.; Pawlus, S.; Zioło, *J. Chem. Phys.* **2005**, *122* (6), 061102.
(56) Root, L. J.; Berne, B. J. *J. Chem. Phys.* **1997**, *107* (11), 4350–4358.
(57) Ngai, K. L.; Casalini, R.; Capaccioli, S.; Paluch, M.; Roland, C. M. *J. Phys. Chem. B* **2005**, *109* (37), 17356–17360.
(58) Hensel-Bielowka, S.; Paluch, M.; Ngai, K. L. *J. Chem. Phys.* **2005**, *123* (1), 014502.
(59) Paluch, M.; Casalini, S.; Hensel-Bielowka, S.; Roland, C. M. *J. Chem. Phys.* **2002**, *116* (22), 9839–9845.
(60) Grzybowska, K.; Pawlus, S.; Mierzwa, M.; Paluch, M.; Ngai, K. L. *J. Chem. Phys.* **2006**, *125* (14), 144507.
(61) Roland, C. M.; Casalini, R.; Paluch, M. *Chem. Phys. Lett.* **2003**, *367* (3−4), 259–264.
(62) Paluch, M.; Rzoska, S. J.; Habdas, P.; Ziolo, J. *J. Phys.: Condens. Matter* **1996**, *8* (50), 10885–10890.
(63) Paluch, M.; Ziolo, J.; Rzoska, S. J.; Habdas, P. *J. Phys.: Condens. Matter* **1997**, *9* (25), 5485–5494.
(64) Andersson, S. P.; Andersson, O. *Macromolecules* **1998**, *31* (9), 2999–3006.
(65) O'Reilly, J. M. *J. Polym. Sci.* **1962**, *57* (165), 429–444.
(66) Atake, T.; Angell, C. A. *J. Phys. Chem.* **1979**, *83* (25), 3218–3223.
(67) Casalini, R.; Roland, C. M. *J. Chem. Phys.* **2003**, *119* (22), 11951–11957.
(68) Casalini, R.; Paluch, M.; Roland, C. M. *J. Phys. Chem. A* **2003**, *107* (13), 2369–2373.
(69) Pawlus, S.; Paluch, M.; Ziolo, J.; Roland, C. M. *J. Phys.: Condens. Matter* **2009**, *21* (33), 332101.
(70) Konishi, T.; Tanaka, H. *Phys. Rev. B.* **2007**, *76* (22), 220201.
(71) Havriliak, S.; Negami, S. A complex plane representation of dielectric and mechanical relaxation processes in some polymers. *Polymer* **1967**, *8* (4), 161.
(72) Rengarajan, G. T.; Beiner, M. *Lett. Drug Des. Discovery* **2006**, *3* (10), 723–730.
(73) Jiménez-Ruiz, M.; Ezquerra, T. A.; Sics, I.; Fernández-Díaz, M. T. *Appl. Phys. A* **2002**, *74* (Suppl. 1), S543−S545.
(74) Sanz, A.; Jiménez-Ruiz, M.; Nogales, A.; Martín y Marero, D.; Ezquerra, T. A. *Phys. Rev. Lett.* **2004**, *93* (1), 015503.
(75) D'Amore, A.; Kenny, J. M.; Nicolais, L.; Tucci, V. *Polym. Eng. Sci.* **1990**, *30*, 314.
(76) Avrami, M. *J. Chem. Phys.* **1939**, *17*, 1103.
(77) Avrami, M. *J. Chem. Phys.* **1940**, *8*, 212.
(78) Wunderlich, B. Macromolecular Physics. *Crystal Nucleation, Growth, Annealing*; Academic Press: London, 1976; Vol. 2.
(79) Avramov, I.; Avramova, K.; Russel, C. *J. Cryst. Growth* **2005**, *285* (3), 394–399.
(80) Napolitano, S.; Wübbenhorst, M. *J. Non-Cryst. Solids* **2007**, *353* (47−51), 4357–4361.
(81) Matsuoka, S. *J. Polym. Sci.* **2003**, *42* (140), 511–524.
(82) Fuss, T.; Ray, C. S.; Kitamura, N.; Makihara, M.; Day, D. E. *J. Non-Cryst. Solids* **2003**, *318* (1−2), 157–167.
(83) Gutzow, I.; Durschang, D.; Russel, C. *J. Mater. Sci.* **1997**, *32* (20), 5389–5403.
(84) Comez, L.; Corezzi, S.; Fioretto, D.; Kriegs, H.; Best, A.; Steffen, W. *Phys. Rev. E* **2004**, *70*, 011504.
(85) Van Krevelen, W. *Properties of Polymers*; Elsevier: Amsterdam, The Netherlands, 1997.
(86) Dymond, J. H.; Malhotra, R. *Int. J. Thermophys.* **1988**, *9* (6), 941–951.

(87) Okumura, T.; Ishida, M.; Takayama, K.; Otsuka, M. *J. Pharm. Sci.* **2006**, *95* (3), 689–700.
(88) Grant, D. J. W. Higuchi, T. *Solubility behavior of organic Compounds*, 1st ed.; John Wiley & Sons: New York, 1990.
(89) Englebert, G.; Beyer, G.; Abdallah, O. *Pharm. Ind.* **1982**, *44*, 1071.
(90) http://www.ccdc.cam.ac.uk.
(91) Rasenack, N.; Muller, B. W. *Drug Dev. Ind. Pharm.* **2002**, *28* (9), 1077–1089.
(92) Garekani, H. A.; Sadeghi, F.; Badiee, A.; Mostafa, S. A.; Rajabi-Siahboomi, A. R. *Drug Dev. Ind. Pharm.* **2001**, *28* (8), 803–809.

JP910009B